Hindawi
Advances in Materials Science and Engineering
Volume 2019, Article ID 9262438, 7 pages
https://doi.org/10.1155/2019/9262438

Research Article

Experimental Verification of Impact of Sprinkled Area Length on Heat Exchange Coefficient

Petr Kracik, Marek Balas, Martin Lisy, and Jiri Pospisil

Department of Power Engineering, Energy Institute, Brno University of Technology, Technická 2896/2, Brno 616 69, Czech Republic

Correspondence should be addressed to Petr Kracik; kracik@fme.vutbr.cz

Received 28 October 2018; Revised 19 February 2019; Accepted 14 March 2019; Published 1 April 2019

Academic Editor: Guang-xing Liang

On a sprinkled tube bundle, liquid forms a thin liquid film, and, in the case of boiling liquid, the liquid phase can be quickly and efficiently separated from the gas phase. There are several effects on the ideal flow mode and the heat transfer from the heating to the sprinkling liquid. The basic quantity is the flow rate of the sprinkling liquid, but also diameter of the tubes, pipe spacing of the tube bundle, and physical state of the sprinkling and heating fluid. Sprinkled heat exchangers are not a new technology and studies have been carried out all over the world. However, experiments (tests) have always been performed under strict laboratory conditions on one to three relatively short tubes and behaviour of the flowing fluid on a real tube bundle has not been taken into account, which is the primary aim of our research. In deriving and comparing the results among the studies, the mass flow rate based on the length of the sprinkled area is used, thus trying to adjust the different length of the heat exchanger. This paper presents results of atmospheric pressure experiments measured on two devices with different lengths of the sprinkled area but with the same number of tubes in the bundle with same pitch and surface at a temperature gradient of 15/40°C, where 15°C is the sprinkling water temperature at the outlet of the distribution pipe and 40°C is the temperature of heating water entering the bundle.

1. Introduction

A horizontal tube bundle, with a formed thin liquid film, is used in various technological processes. The main asset is the fact that the vapour phase of the sprinkling liquid may quickly and efficiently be separated from the liquid phase; this is in contrast to the boiling of large-volume liquids. This situation enhances the efficiency of heat transfer from a heated tube into the sprinkling liquid. The technology is commonly used for distillation of salt water. Thanks to the sprinkled exchangers, the process may occur under relatively low temperatures (tens of Celsius degrees). However, the ambient pressure must adequately be decreased in order to achieve the boiling point. Low-potential heat from various power processes, geothermal springs, solar panels, and others may serve as a source of heating for the liquid boiling.

Ideally, the sprinkling liquid boils evenly on the whole surface of the exchanger. However, in practice, the initial contact of the liquid with the exchanger walls does not lead to boiling on the tube surface and only causes heating of the sprinkling liquid. The liquid current acts similarly as the condensation of water vapour in the vertical pipe. From a hydraulic point of view, the process is described in [1] for clean water, and in [2] for water mixture (water vapour and air).

Mass flow rate related to length $\Gamma\,(\mathrm{kg{\cdot}s^{-1}{\cdot}m^{-1}})$ is commonly used to assess the measured data. The flow rate of sprinkling liquid on the tube wall, provided that it has been stabilised and has a constant downstream thickness $\delta\,(\mathrm{m})$, may be described using [3] as an integration of the equation of motion:

$$\Gamma = \frac{\rho \cdot g}{\nu} \cdot \frac{\delta^3}{3} \left(\mathrm{kg{\cdot}s^{-1}{\cdot}m^{-1}}\right), \tag{1}$$

where $\rho\ (\mathrm{kg{\cdot}m^{-3}})$ is the density of the liquid, $g\,(\mathrm{m{\cdot}s^{-2}})$ is the acceleration caused by gravity, and $\nu\,(\mathrm{m^2{\cdot}s^{-1}})$ is the

kinematic viscosity of the liquid. The mass flow rate Γ may also be identified using the measured volumetric flow rate $\dot{V}$ ($m^3 \cdot s^{-1}$) multiplied by density ρ ($kg \cdot m^{-3}$) of the sprinkling liquid, which reflects the current state of the liquid, and divided by the length of the sprinkled area L (m) (length of the distribution tube):

$$\Gamma = \frac{\dot{V} \cdot \rho}{L} \left(kg \cdot s^{-1} \cdot m^{-1} \right). \quad (2)$$

According to [4–6], the Reynolds number is given as follows:

$$\mathrm{Re} = \frac{4 \cdot \Gamma}{\mu} (-), \quad (3)$$

where μ ($Pa \cdot s$) is the dynamic viscosity of liquid film. Based on the given Reynolds number, it is possible to describe the mode of sprinkling that the liquid creates on the horizontal tube bundle. The modes are shown in Figure 1, and they are (a) a drop mode, (b) jet (column) mode, and (c) sheet mode. Definitions and semiempirical relations describing individual modes are, for example, in [8–10]. Except for the sprinkling mode, equations depending on the Reynolds number for flow modes (laminar and turbulent) are also derived, for example, [3, 11].

Physical models of heat transfer from heating fluid through the walls of the tube bundle into liquid film flowing down the bundle can be divided into three basic groups that have been published over time. The result is either the Nusselt number (Nu (−)) or the heat transfer coefficient of the flowing liquid α_o ($W \cdot m^{-2} \cdot K^{-1}$). The conversion for a thin liquid film flowing down the tube bundle is

$$Nu = \alpha \cdot \sqrt[3]{\frac{\nu^2}{g \cdot \lambda^3}} = \alpha \cdot \sqrt[3]{\frac{\mu^2}{g \cdot \rho^2 \cdot \lambda^3}} (-), \quad (4)$$

where λ ($W \cdot m^{-1} \cdot K^{-1}$) is the thermal conductivity of the flowing liquid. Equations for water, as liquid flowing down the tube bundle, for practical use of experimental results have been generalised by Chun and Seban [3]. This model was followed by heating [12, 13], but it was still only a simplified model not distinguishing the individual phases: heating of the liquid, start and full boil liquid on the bundle. These complex models were developed only for one horizontal tube on which the ideal liquid film was created. Derived semiempirical relations are described in [14–17]. The third mathematical model uses the superposition principle and can be used not only for water but also for refrigerants, thanks to the Martinelli parameter. The model definition is presented in [11].

2. Measurement Apparatus

Experiments published in this paper were performed on two experimental devices, designed at the Department of Power Engineering. An atmospheric stand (AS) is one of them. The stand was designed to test optimum amount of tubes in the bundle, their pitch, and the tube bundle surface with regard to relative simplicity of the tested bundle construction. A vacuum stand (PS) is the other device established at the Department. Commissioning and construction of the tube bundle are complicated (the bundle has to be soldered), and the objective of the experiments is to identify the impact of the external pressure on the heat transfer and temperature distribution in an 8-tube bundle with 20.0 mm tube pitch. The tube with a copper surface is smooth (no treatments), and only top four or six tubes may be heated.

Two metal sheets with holes drilled in them encompass the sprinkled area. Sprinkled tubes together with a distribution tube above it are placed into these holes. The diagram of the tube bundle with a description of measured physical quantities is shown in Figure 2. With regard to the vacuum chamber design, the length of the sprinkled area had to be reduced from 1000 mm (length of the area for experiments in the atmospheric stand) to 940 mm. Orifices, with diameters ranging from 1.0 mm to ca. 9.2 mm, are drilled into the distribution tubes in both stands. The initial and final orifices are drilled ca. 10.0 mm apart from the metal sheet. The vacuum stand (PS) has 100 orifices; the atmospheric stand (AS) has 107 orifices. The sprinkling liquid flows from these orifices.

Two common loops are connected to the vacuum stand (PS) and the atmospheric stand (AS): heating loop and sprinkling loop. The heating liquid flowing inside the tubes is intended for overpressure of up to 1.0 MPa. The sprinkling loop contains falling liquid film. There is a pump, regulation valve, flow meter, and plate heat exchangers attached to both loops. The plate heat exchanger at the heating loop is connected to a gas boiler which supplies heat to the heating liquid. The sprinkling loop uses two plates of heat exchangers. In the first heat exchanger, the falling film liquid is cooled by cold drinkable water from water mains and the falling film liquid is cooled in the other heat exchanger with drinkable water cooled in a cooler which regulates the temperature up to 1.0°C. In order to enable visual control, the heating loop also includes a manometer and thermometer. The thermal status in individual loops is measured by using wrapped unearthed T-type thermocouples on the agents' input and output from the vessel. All thermocouples have been calibrated in the CL1000 Series calibration furnace which maintains a given temperature with the accuracy ±0.15°C. None of the thermocouples has exceeded the error ±0.5°C within the studied range from 28°C to 75°C. That is why the total error at temperature measurement is set uniformly for all thermocouples along the whole studied range at ±0.65°C.

Electromagnetic flow meters Flomag 3000 attached to both loops measure the flow rate. The flow meters' range is $0.0078/0.9424\,l \cdot s^{-1}$, where the accuracy is 0.5% from the measured range, that is, $\pm 0.004\,67\,l \cdot s^{-1}$. All examined quantities are either directly (thermocouples) or via transducers scanned by measuring cards DAQ 56 with the frequency of 0.703 Hz.

3. Methodology of Data Assessment

The assessment of the measured data is based on the thermal balance between the operation liquid circulating inside the tubes and sprinkling loop according to the law of

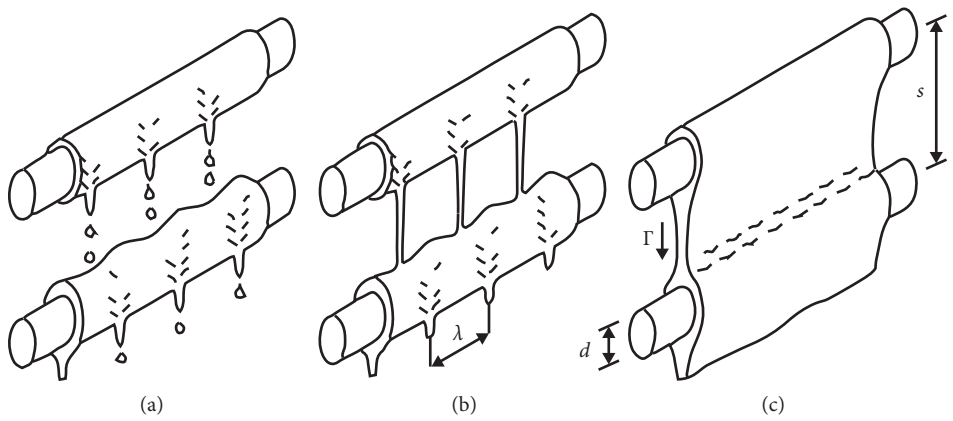

Figure 1: Sprinkling modes [7]. (a) Drop. (b) Jet (column). (c) Sheet.

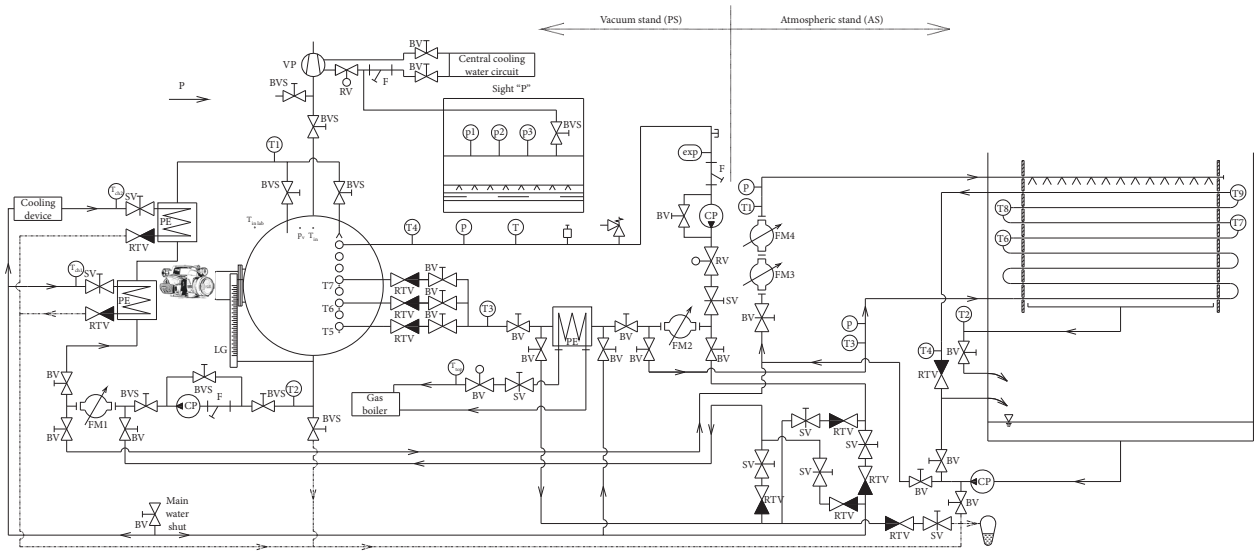

Figure 2: Simplified diagram of the experimental device with description of measured quantities.

conservation of energy. Heat transfer is realized by convection, conduction, and radiation. At lower temperatures, the heat transferred by radiation is negligible; therefore, it is excluded from further calculations. The calculation of the studied heat transfer coefficient is based on Newton's heat transfer law and Fourier's heat conduction law that have been used to form the following equation:

$$\alpha_o = \frac{1}{2 \cdot \pi \cdot r_o \cdot \left[\left(1/k_S\right) - \left(1/2 \cdot \pi \cdot \alpha_i \cdot r_i\right) - \left(1/2 \cdot \pi \cdot \lambda_S\right) \cdot \ln\left(r_o/r_i\right)\right]}, \quad (5)$$

where $\alpha_o\,(\mathrm{W \cdot m^{-2} \cdot K^{-1}})$ is the heat transfer coefficient at the sprinkled tubes' surface, $\alpha_i\,(\mathrm{W \cdot m^{-2} \cdot K^{-1}})$ is the heat transfer coefficient at the inner side of a tube set for a fully developed turbulent flow according to [18], r_o and $r_i\,(\mathrm{m})$ are the outer and inner tube radii, $\lambda_S\,(\mathrm{W \cdot m^{-1} \cdot K^{-1}})$ is thermal conductivity, and $k_S\,(\mathrm{W \cdot m^{-1} \cdot K^{-1}})$ is the heat admittance based on the abovementioned laws governing heat transfer which is calculated from heat balance of the heating side of the loop, that is why the following must be valid:

$$\dot{Q}_S = k_S \cdot L \cdot \Delta T_{\ln} = \dot{M}_{34} \cdot c_p\left(\frac{t_3 + t_4}{2}\right) \cdot \left(t_3 - t_4\right), \quad (6)$$

where $\dot{M}_{34}\,(\mathrm{kg \cdot s^{-1}})$ is the mass flow of heating water, $c_p\,(\mathrm{J \cdot kg^{-1} \cdot K^{-1}})$ is the specific heat capacity of water at constant pressure related to the mean temperature inside the loop, $L\,(\mathrm{m})$ is the total length of the bundle, and $\Delta T_{\ln}\,(K)$ is a logarithmic temperature gradient where a countercurrent exchanger was considered.

4. Experiment Results

For comparison, two experiments were selected. Both were performed under 15/40 temperature gradient and $5.0\,\mathrm{L \cdot min^{-1}}$ sprinkling liquid flow rate in the tube bundle consisting of six tubes. As for the vacuum stand, the average

temperature of the sprinkling water at the outlet from the distribution tube was $t_1 = 15.1 \pm 0.1^{\circ}C$, and the average flow rate was $\dot{V}_1 = 5.02 \pm 0.01\,L{\cdot}min^{-1}$. As for the atmospheric stand, the average temperature of the sprinkling water at the outlet from the distribution tube was $t_1 = 14.5 \pm 0.1^{\circ}C$, and the average flow rate was $\dot{V}_1 = 4.99 \pm 0.02\,L{\cdot}min^{-1}$. In the vacuum stand, the average temperature of heating water entering the tube bundle was $t_3 = 40.2 \pm 0.1^{\circ}C$, and the average flow rate was $\dot{V}_2 = 7.15 \pm 0.01\,L{\cdot}min^{-1}$. In the atmospheric stand, the average temperature was $t_3 = 40.2 \pm 0.4^{\circ}C$, and the average flow rate was $\dot{V}_2 = 7.16 \pm 0.06\,L{\cdot}min^{-1}$.

Figure 3(a) shows changes in temperature of the heating water flowing in the bundle (this is designated as "PS_i" for the vacuum stand and "AS_i" for the atmospheric stand) in relation to the length of the sprinkled area. Changes in the temperature of the sprinkling liquid (designated as "PS_o" for the vacuum stand and "AS_o" for the atmospheric stand) are depicted in Figure 3(b). Changes in the heating water temperature are depicted using straight lines to show real flows inside the tube bundle; that is, water enters the bundle in the bottom most tube and moves upward. In the atmospheric stand, temperatures at the outlet from one tube/inlet to the other tube were also measured (in addition to inlet and outlet temperatures). Mean temperature of the heating water (temperature in the middle of the tube) was calculated as an average inlet and outlet temperatures of the given tube. In the vacuum stand, the temperature between the penultimate tube (no. 5) and the last tube (no. 6) was not measured. Therefore, the temperature was calculated using linear interpolation; in other words, it is the temperature of the heating water entering the bundle and the temperature of the heating water leaving the tube no. 5 (entering tube no. 4). Mean temperature in the middle of these two tubes was calculated using the said temperature.

Changes in the temperature in particular tubes may be described using a gradient of a line. It is the difference in the temperature of the heating water entering the tube and temperature of the heating water leaving the tube, divided by the length of the tube. In the atmospheric stand, the gradient of a line rises from the last tube to the first tube, from $1.3^{\circ}C{\cdot}m^{-1}$ to $3.4^{\circ}C{\cdot}m^{-1}$, with a mild slowdown at tube nos. 2 and 4. Changes in temperature are similar for the vacuum stand. The gradient of a line is identical for the last two tubes, that is, $1.6^{\circ}C{\cdot}m^{-1}$. This is caused by the division of the same temperature gradient using linear interpolation for these two tubes. Otherwise, the temperature changes are relatively similar. The gradient of a line is $3.2^{\circ}C{\cdot}m^{-1}$ (first tube), with a mild slowdown on tube no. 2. Differences of gradients of the line are not significant. However, if medium temperature differences (that is the average temperature related to the centre of the given tube) of particular bundles are compared, one can observe temperature increase of up to $1.22^{\circ}C$ on the first tube (the atmospheric stand). Changes in differences of medium temperatures (Dt) in relation to the number of the tube are given in Figure 3(b).

Figure 3(b) shows the calculated heat fluxes of a sampled heating liquid in individual tubes. Tube no. 6 is the only one where heat flow is higher for the vacuum stand. Even distribution of medium temperature is probably an important factor here as well. The heat flow in all other tubes is higher in the atmospheric stand, with the only exception of tube no. 4 where heat flows are even. The chart also shows slowdown of temperature changes which have been described above.

Figures 4 and 5 illustrate the impact of sprinkled area length for 4-, 6-, and 8-tube bundle and various sprinkling liquid flow rates. Table 1 presents basic information about given areas. The scope of sprinkling liquid flow rate in the atmospheric stand ranges from 1.3 to $13.6\,L{\cdot}min^{-1}$. This corresponds to the scope of mass flow related to the sprinkled area length (Γ) 0.021 to $0.227\,kg{\cdot}s^{-1}{\cdot}m^{-1}$. As for the vacuum stand, scope of sprinkling liquid flow rate ranges only from 3.4 to $8.1\,L{\cdot}min^{-1}$; that is, the mass flow rate related to the sprinkled area length ranges from 0.060 to $0.144\,kg{\cdot}s^{-1}{\cdot}m^{-1}$.

Figure 4 compares heat transfer coefficient to the sprinkled tube bundle surface in relation to the specific heat input taken from the heating liquid. Temperature changes of the 4-tube bundle are given in Figure 4(a) (dark blue represents the vacuum stand). In Figure 4(b), there are values for 6-tube bundle (in green). In Figure 4(c), there are values for 8-tube bundle (dark colour for the vacuum stand and orange for the atmospheric stand). All three cases present roughly linear trends, and values determined for vacuum stand copy changes of values determined for the atmospheric stand.

Figure 5 illustrates the identical values of heat transfer coefficient in relation to a mass flow rate of the sprinkling liquid related to sprinkled area length. Heat transfer coefficients are again presented in three charts and the same colours as in Figure 4. To make the trends more obvious, particular patterns were marked with a curve. All curves are in black. The differences are most prominent for a 4-tube bundle. The difference of the coefficient at the smallest flow rate of the sprinkling liquid is ca. 10%; increase in flow rate results in an increase in the difference to ca. 32% at a flow rate of ca. $6.0\,L{\cdot}min^{-1}$. The last and highest coefficient value (in vacuum stand experiments) is determined for the flow rate of ca. $8.0\,L{\cdot}min^{-1}$ and coefficient difference of ca. 16%. For the 6-tube bundle, the coefficient trend for the vacuum stand copies the coefficient trend for the atmospheric stand, including the coefficient drop. Differences in the heat transfer coefficient ranged from ca. 15–32%. As for the 8-tube bundle, the results determined for both devices are not unequivocal. At the flow rate of ca. $3.6\,L{\cdot}min^{-1}$, the values for the vacuum stand are higher by ca. 27% (compared to the AS curve). At the flow rate of ca. $4.7\,L{\cdot}min^{-1}$, the coefficient for vacuum and atmospheric stands reaches identical values. For the highest measured flow rate, the difference of the coefficient reaches ca. 12% (the coefficient is higher in the vacuum stand).

In Figure 5, the heat transfer coefficient values are compared with the three mathematical models derived for the sprinkling liquid that is heated on the surface of the tube bundle or is kept on the boiling sublimation point; i.e., the liquid is in a saturation state but does not yet boil. The first model was published by Parken et al. [12], based on experiments carried

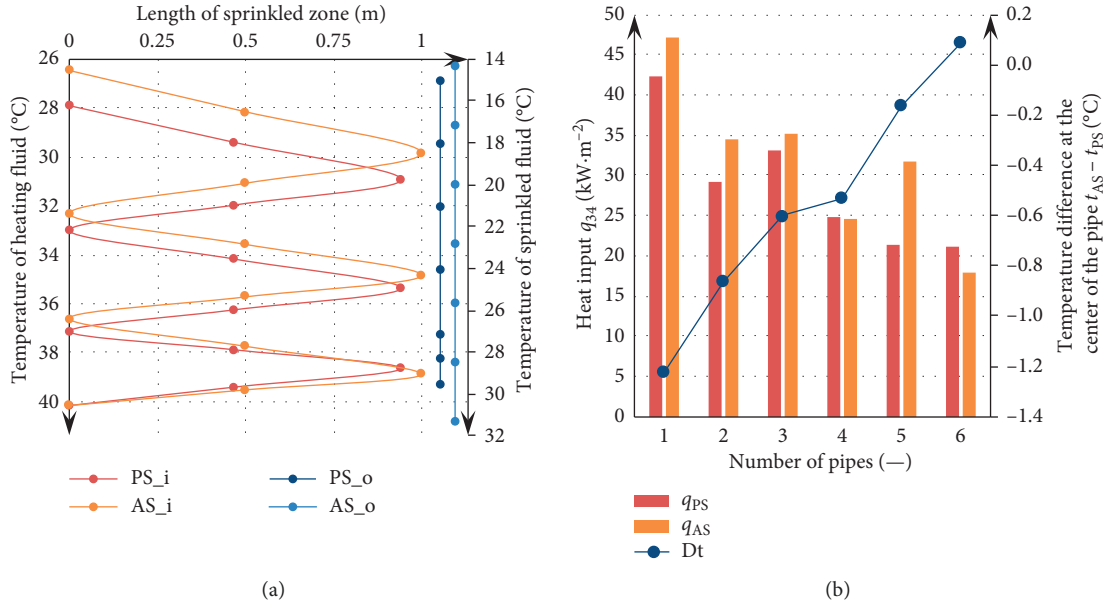

Figure 3: Impact of sprinkled area length on temperature changes of heating liquid in loop (a) and on sampled heat flux (b).

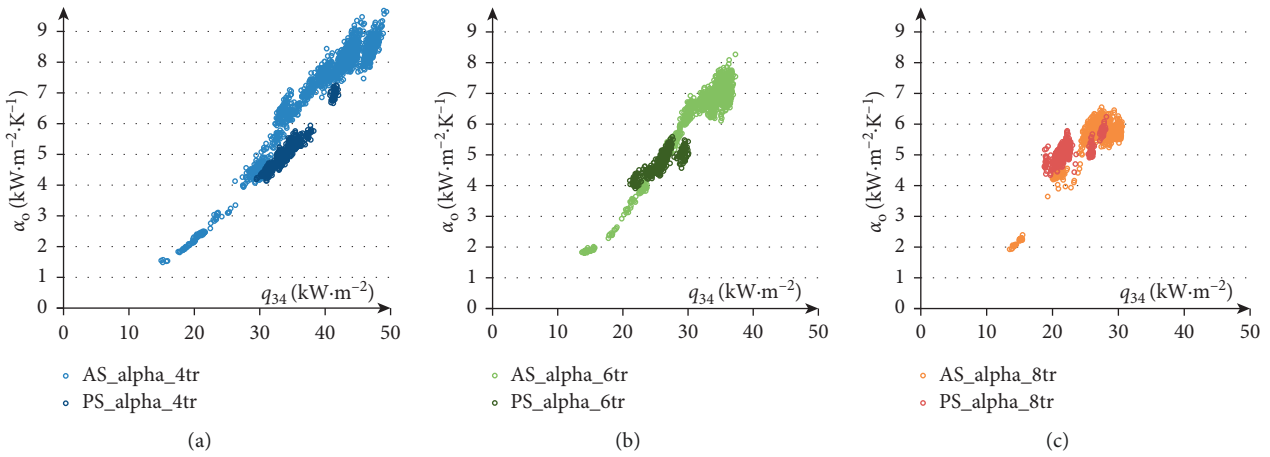

Figure 4: Comparison of heat transfer coefficient in relation to heat input.

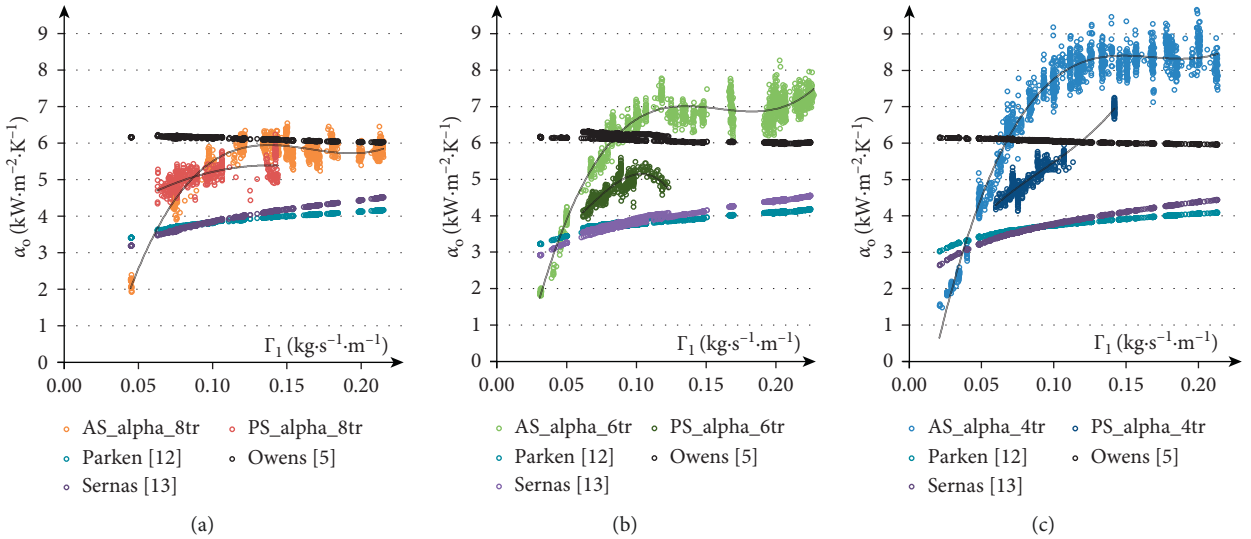

Figure 5: Comparison of heat transfer coefficients in relation to mass flow rate.

Table 1: Overview of basic measured and derived quantities.

Number of tubes	t_1 (°C)	t_2 (°C)	$\dot{V}_1$ (L·min^{-1})	Re (–)	t_3 (°C)	t_4 (°C)	$\dot{V}_2$ (L·min^{-1})
Atmospheric stand (AS)							
4	14.8 ± 0.4	27.1 ± 3.5	1.3–12.8	91.7–819.3	40.2 ± 0.4	28.3 ± 2.3	7.22 ± 0.05
6	14.7 ± 0.5	27.3 ± 3.5	1.9–13.6	138.4–910.6	39.8 ± 0.4	25.1 ± 2.2	7.20 ± 0.05
8	14.7 ± 0.5	29.0 ± 2.5	2.7–12.9	199.4–868.6	40.4 ± 0.5	23.9 ± 1.8	7.20 ± 0.06
Vacuum stand (PS)							
4	15.3 ± 0.4	28.7 ± 1.5	3.4–8.0	262.0–574.4	40.1 ± 0.4	30.3 ± 0.9	7.18 ± 0.02
6	15.1 ± 0.5	29.8 ± 1.1	3.5–7.0	275.3–519.0	40.1 ± 0.4	29.0 ± 0.8	7.15 ± 0.01
8	15.2 ± 0.5	34.3 ± 2.4	3.6–8.1	285.0–614.4	40.3 ± 0.4	27.4 ± 1.3	7.16 ± 0.03

out on an electrically heated brass tube. The experiments were done at a temperature range of 45.0–127.0°C and a mass flow rate of 0.135–0.366 kg·s^{-1}·m^{-1}. The second model is from the study of Sernas [13]. He also conducted experiments on one electrically heated brass pipe at a sprinkling liquid (water) temperature range of 44.9 − 117.0°C and a mass flow range of 0.133 − 0.292 kg·s^{-1}·m^{-1}. In both cases, the experiments were performed on one and two inch tubes, and for each diameter, they expressed the Nusselt number, depending on the Reynolds and Prandtl numbers. For comparison, the Nusselt number equation for the 1″ dimension was used.

Although both studies indicate that they did not find a significant dependence on the Reynolds number, it should be noted that the results for AS and PS were determined within the mass flow rate of the sprinkling liquid 0.021 − 0.227 kg·s^{-1}·m^{-1} and 0.060 − 0.144 kg·s^{-1}·m^{-1}. From this perspective, the equations are valid for approximately the second half of the carried out (compared) experiments. In the comparison of the AS and PS experiment results, the average temperatures of the sprinkling liquid are dependent on the size of its flow and in the range of about 18.2 − 25.2°C, which is below the lower limit of mathematical models with which data are compared. The result is a slightly higher Prandtl number introduced into the criterial equations to determine the Nusselt number.

The third mathematical model is according to Owens [5]. He conducted experiments on an electrically heated smooth steel tube, where he also tested the distance of the distribution pipe. Therefore, in the criterial equations, a constituent taking into account the ratio of pitch difference and tube diameter to tube diameter is used. Also, the criterial equations were divided according to the flow regime (laminar and turbulent). For comparison, the Nusselt number equation for the turbulent flow mode, the whole of which corresponds to the compared data, was used.

The Reynolds and Prandtl numbers were entered into all three criterial equations defined by the authors mentioned. These numbers were derived based on the data obtained from individual experiments. The best match was achieved for the eight-tube bundle with AS with the progression determined by Owens. The difference between the mean values of the heat transfer coefficient was about 4.7% at a flow rate higher than about 0.11 kg·s^{-1}·m^{-1}. For both four-tube and six-tube bundles, the flow limit has dropped, which can be considered to be the heat transfer coefficient development relatively independent of the sprinkling liquid flow rate of about 0.1 kg·s^{-1}·m^{-1}.

For the six- and four-tube bundle, the coefficient of heat transfer stated according to Owens remained at approximately the same level. However, the developments of the coefficient derived from the experiments, when increasing the specific load, this development skipped, and the mean difference is about 11% higher in the case of a six-tube bundle; the case of a four-tube bundle volume is about 25% higher.

Undershoot of the flow limits is mentioned in the particular geometries in the previous paragraph, the heat transfer coefficient determined by the experiments decreased rapidly, and the developments intersect with the remaining compared developments which were determined in the studies of Parken and Sernas. In all three graphs, the Parken and Sernas developments are at about the same level. The variance of the average value determined from the individual values calculated at the same flow rate is at higher flow rates about 5.2%, and with the decreasing flow rate, the variance increases. At the lowest measured flow rate in the case of a four-pipe bundle, the variance reaches up to 8.6%.

The steep decrease in the heat transfer coefficient of the small sprinkle liquid flow rates that occurred when the above flow limits of the AS experiments undershot could be caused by too thin a liquid film and a relatively small sampling of heating fluid heat flows. Ganic and Roppo [19] calls this a "dryout," although dry places are not present on the bundle, and therefore, for example, Ribatski and Thome [20] calls it "nondryout." The experiments presented were completed at the latest when the first dry spot appeared on the bundle, which was well detectable by an infrared camera.

The results of the PS experiments varied between developments determined by Owens, where higher values were achieved over the whole range compared, and conversely, the Perken and Sernas courses were in the lower range throughout the whole compared range. From this point of view, the coefficient values for the four- and eight-tube bundle were closest at the highest measured flow rate to that of Owens. In the four-tube bundle, the mean value obtained from the experiments was about 8.0% smaller, and for the eight-tube bundle, the mean value was about 10.0% smaller, with several values at the level of this compared development.

5. Conclusion

The objective of this paper was to compare the tube bundle sprinkled areas of various lengths that comprise 4/6/8 tubes. Experiments were performed on two devices. One of them

was the atmospheric stand with sprinkled area length of 1000 mm. The other was the vacuum stand with sprinkled area length of 940 mm. Other parameters, such as bundle geometry, flow rate of sprinkling and heating liquids, and liquids' temperature at the outlet/inlet to the exchanger, were roughly similar. Temperature changes of the heating liquid for both devices with 6-tube exchanger are given for 15/40°C temperature gradient and sprinkling liquid flow rate of ca. 5.0 $L \cdot min^{-1}$. It seems that the longer sprinkled area is more promising since the gradients of a line for temperature in tubes are roughly identical. Figure 4 shows heat transfer coefficients to the sprinkled tube bundle surface for three arrangements of tubes at various flow rates of sprinkling liquid in relation to specific heat input of the heating liquid. All three cases present roughly linear trends, and values determined the for vacuum stand roughly copy values determined for the atmospheric stand.

Figure 5 illustrates heat transfer coefficient in relation to the mass flow rate of sprinkling liquid related to sprinkled area length. Charts prove that mass flow rate does not compensate for different lengths of the sprinkled area since heat transfer coefficient was lower by ca. 32% for the shorter bundle. Therefore, when using the recommended semi-empirical relations for calculating the heat transfer coefficient or the Nusselt numbers, it is necessary to take into account the experimental devices from which these were derived.

In conclusion, the presented values were compared with other authors. However, it is only necessary to consider the comparison as a guide, for several reasons. The authors investigated the heat transfer coefficient on one short electrically heated tube up to 1 meter long, with 1″ and 2″ in diameter, made of brass or stainless steel. The most significant concordance was reached with the compared results obtained on the AS of the eight-tube bundle. However, none of the mathematical models considered a sharp decrease in the heat transfer coefficient of a thin film of the sprinkling liquid on a bundle that draws a low heat flow.

Data Availability

All originally presented data used to support the findings of this study are available from the corresponding author upon request.

Conflicts of Interest

The authors declare that they have no conflicts of interest.

Acknowledgments

This work was supported by the Ministry of Education, Youth and Sports of the Czech Republic under OP RDE grant number CZ.02.1.01/0.0/0.0/16_019/0000753 "Research Centre for Low-Carbon Energy Technologies."

References

[1] J. Havlík and T. Dlouhý, "Condensation of water vapor in a vertical tube condenser," *Acta Polytechnica*, vol. 55, no. 5, pp. 306–312, 2015.

[2] J. Havlík and T. Dlouhý, "Condensation of the air-steam mixture in a vertical tube condenser," *EPJ Web of Conferences*, vol. 114, p. 02037, 2016.

[3] K. R. Chun and R. A. Seban, "Heat transfer to evaporating liquid films," *Journal of Heat Transfer*, vol. 93, no. 4, pp. 391–396, 1971.

[4] X. Hu and A. M. Jacobi, "The intertube falling film: part 2-mode effects on sensible heat transfer to a falling liquid film," *Journal of Heat Transfer*, vol. 118, no. 3, pp. 626–636, 1996.

[5] W. Owens, "Correlation of thin film evaporation heat transfer coefficients for horizontal tubes," in *Proceedings of the Fifth Ocean Thermal Energy Conversion Conference*, pp. 71–89, Miami Beach, FL, USA, February 1978.

[6] J. Lorenz and D. Yung, "Combined boiling and evaporation of liquid films on horizontal tubes," in *Proceedings of the Fifth Ocean Thermal Energy Conversion Conference*, pp. 46–69, Miami Beach, FL, USA, February 1978.

[7] R. Armbruster and J. Mitrovic, "Evaporative cooling of a falling water film on horizontal tubes," *Experimental Thermal and Fluid Science*, vol. 18, no. 3, pp. 183–194, 1998.

[8] F. A. Jafar, G. R. Thorpe, and Ö. F. Turan, *Computational Fluid Dynamics Seventh International Conference on CFD in the Minerals and Process Industries*, CSIRO, Melbourne, VIC, Australia, 2009.

[9] R. Armbruster and J. Mitrovic, "Patterns of falling film flow over horizontal smooth tubes," in *Proceedings of the 10th International Heat Transfer Conference*, vol. 3, pp. 275–280, Brighton, UK, August 1994.

[10] J. F. Roques, V. Dupont, and J. R. Thome, "Falling film transitions on plain and enhanced tubes," *Journal of Heat Transfer*, vol. 124, no. 3, pp. 491–499, 2002.

[11] L.-H. Chien and C.-H. Cheng, "A predictive model of falling film evaporation with bubble nucleation on horizontal tubes," *HVAC&R Research*, vol. 12, no. 1, pp. 69–87, 2006.

[12] W. H. Parken, L. S. Fletcher, V. Sernas, and J. C. Han, "Heat transfer through falling film evaporation and boiling on horizontal tubes," *Journal of Heat Transfer*, vol. 112, no. 3, pp. 744–750, 1990.

[13] V. Sernas, "Heat transfer correlation for subcooled water films on horizontal tubes," *Journal of Heat Transfer*, vol. 101, no. 1, pp. 176–178, 1979.

[14] J. J. Lorenz and D. Yung, "A note on combined boiling and evaporation of liquid films on horizontal tubes," *Journal of Heat Transfer*, vol. 101, no. 1, pp. 178–180, 1979.

[15] W. M. Rohsenow, "Discussion: "on the rohsenow pool-boiling correlation" (Frost C. W., and Li K. W., 1971, ASME J. Heat Transfer, 93, pp. 232–234)," *Journal of Heat Transfer*, vol. 94, no. 2, pp. 255-256, 1972.

[16] M. G. Cooper, "Saturation nucleate pool boiling: a simple correlation," in *Proceedings of the First U.K. National Conference on Heat Transfer*, vol. 86, pp. 785–793, Leeds, UK, July 1984.

[17] A. Luke, "Preparation and analysis of different roughness structures for evaporator tubes," *Heat and Mass Transfer*, vol. 45, no. 7, pp. 909–917, 2009.

[18] F. P. Incropera, *Fundamentals of Heat and Mass Transfer*, John Wiley, New York, NY, USA, 6th edition, 2007.

[19] E. N. Ganic and M. N. Roppo, "An experimental study of falling liquid film breakdown on a horizontal cylinder during heat transfer," *Journal of Heat Transfer*, vol. 102, no. 2, pp. 342–346, 1980.

[20] G. Ribatski and J. R. Thome, "Experimental study on the onset of local dryout in an evaporating falling film on horizontal plain tubes," *Experimental Thermal and Fluid Science*, vol. 31, no. 6, pp. 483–493, 2007.